ELSEVIER

Journal of Nuclear Materials 304 (2002) 117–128

journal of nuclear materials

www.elsevier.com/locate/jnucmat

Kinetics of nucleation and coarsening of colloids and voids in crystals under irradiation

V.I. Dubinko [a], A.A. Turkin [a], D.I. Vainshtein [b], H.W. den Hartog [b,*]

[a] National Science Center Kharkov Institute of Physics and Technology, 310108 Kharkov, Ukraine
[b] Solid State Physics Laboratory, University of Groningen, Nijenborgh 4, NL-9747 AG Groningen, The Netherlands

Received 26 February 2002; accepted 30 May 2002

Abstract

The kinetics of nucleation and coarsening of vacancy clusters in irradiated crystals are considered with account of their elastic interaction with point defects resulting in the biased absorption of vacancies and interstitial atoms. It is shown that in the technologically important range of high dose rate (or low temperature) irradiation, the nucleation rate and the final number density of clusters are determined by the bias parameters rather than by irradiation conditions. The model is applied to the evolution of sodium colloids and chlorine bubbles in NaCl resulting in the formation of voids followed by a sudden fracture of the material, which presents a potential problem in rock salt nuclear waste repositories. The number densities and mean sizes of colloids, bubbles and voids are evaluated and compared with experimental data.

PACS: 61.72.Ji; 61.72.Qq; 61.80.Az

1. Introduction

Irradiation of crystals results in the formation of point defects (PD) and their clusters. In metals, radiation-induced defects are voids, gas bubbles and dislocation loops. In ionic crystals, such as alkali halides, irradiation results in the formation of halide 'bubbles' formed by agglomeration of H centers and of the complementary inclusions of metallic 'colloids' formed by agglomeration of F centers [1–3]. H and F centers are the primary radiation defects in the halide sub-lattice, whereas the cation sub-lattice is not damaged in the primary displacement process. The H center is an interstitial halide ion with a trapped hole, and an F center is the vacancy in the halide sub-lattice with a trapped electron. Our experiments on heavily irradiated pure and doped NaCl and natural rock salt samples have shown that with increasing dose, the formation of relatively large voids was observed followed by a sudden fracture of the material [4–8] (Fig. 1). The difficulty to explain void formation in ionic crystals appeared to be the creation of electroneutral vacancy pairs (two adjacent vacancies in the cation and in the anion sub-lattices), since irradiation produces only Frenkel pairs in the halide sublattice. We have proposed a new model [9–11], which involves the production of V_F centers (a cation vacancy with a self-trapped hole) at dislocations as a result of their reaction with H centers. Voids have been shown to arise as a result of collisions of growing metallic colloids with fine stable halogen bubbles [11]. Voids can grow rapidly due to the formation of electroneutral vacancy pairs in the reaction between F centers and V_F centers at their surfaces. The model predicts that voids grow to sizes exceeding the mean distance between bubbles and colloid, eventually absorbing them, and, hence, bringing the halogen gas and metal to a back reaction. This leads

* Corresponding author. Tel.: +31-50 363 4789; fax: +31-50 363 4879.
E-mail address: h.w.den.hartog@phys.rug.nl (H.W. den Hartog).

0022-3115/02/$ - see front matter
PII: S0022-3115(02)00902-9

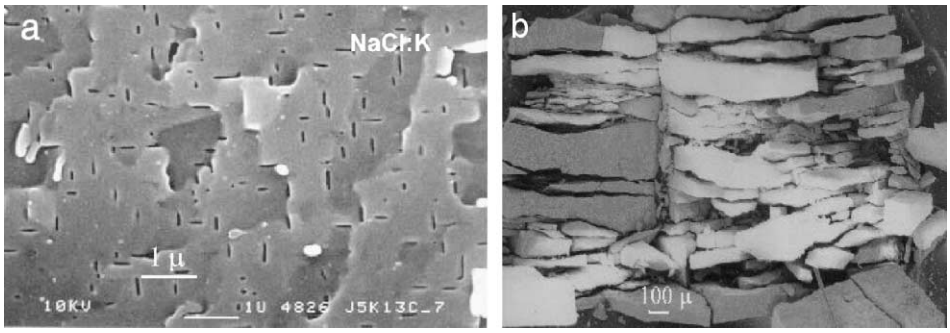

Fig. 1. Effect of irradiation on NaCl + K (0.1 mol%) samples irradiated with 0.5 MeV electrons to 300 Grad at 100 °C: (a) SEM micrographs showing vacancy voids and penny-shaped cracks; (b) SEM micrograph of the exploded sample reveals large fragments and dust-like particles.

to the explosive release of radiation-induced stored energy within the voids and to void-crack transformations [12]. We attribute the destruction of salt samples after high dose irradiation [4–8] to these phenomena.

The sizes and number densities of colloids and bubbles are the factors of primary importance, since they determine both the onset of the void formation (resulting from the collisions between colloids and bubbles) and the onset of the void-crack transition resulting from the collisions between voids and colloids. In earlier contributions [9–11] we have considered the post nucleation stage of microstructure evolution. At that stage, the final number density of colloids was assumed to be equal to the asymptotic maximum value determined by the radiation-induced coarsening (RIC) mechanism in the same way as the number density of voids in irradiated metals [13]. The RIC mechanism is based on the dependence of the colloid bias for H center absorption on the colloid radius so that the large colloids can grow at the expense of small ones, which limits the maximum number density of colloids that can grow under specific irradiation conditions. This maximum number density is proportional to the mean dislocation density and does not depend on the colloid nucleation rate. However, the actual number density of colloids appears to be lower than the maximum value, and the difference between the two depends on the nucleation rate.

In the present paper, we consider the kinetics of nucleation and coarsening of metallic colloids and evaluate the number density and mean size of colloids as a function of irradiation dose.

The paper is organized as follows.

In Section 2, we develop a model of the colloid nucleation under irradiation with account of their elastic interaction with F and H centers, which can also be applied to the nucleation of voids in metals.

In Section 3 we consider the simultaneous nucleation and coarsening of metallic colloids and halogen bubbles at a constant dislocation density, and compare the results with the asymptotic solution.

Void formation and growth in NaCl under irradiation is analyzed and compared with the experimental data in Section 4.

The results are discussed and summarized in Section 5.

2. Nucleation model

2.1. Rate equations

The primary vacancy and interstitial PD, which are produced in alkali halides during exposure to ionizing irradiation, are F and H centers. Their respective mean concentrations $\bar{c}_{F,H}$ are determined by the following rate equations:

$$\frac{d\bar{c}_{F,H}}{dt} = K_{F,H} - k^2_{F,H} D_{F,H}(\bar{c}_{F,H} - \bar{c}^{th}_{F,H}) - \beta_r(D_F + D_H)\bar{c}_F\bar{c}_H, \tag{1}$$

$$k^2_{F,H} = Z^d_{F,H}\rho_d + \sum_S Z^S_{F,H} 4\pi N_S \overline{R}_S, \tag{2}$$

where $K_{F,H}$ is the production rate of F and H centers, usually measured in displacement per atom per second (dpa/s), β_r is the constant of their bulk recombination, $k^2_{F,H}$ are the sink strengths associated with absorption and thermal emission of PD by extended defects (ED), $\bar{c}^{th}$ is the mean concentration of thermal PD, ρ_d is the dislocation density, N_S is the number density of 'spherical' S-type ED's (colloids, bubbles and voids), and $\overline{R}_S$ is their respective mean radius; $Z^S_{F,H}$ are the sink capture efficiencies for the PD's, which determine the microstructure evolution under steady state conditions (i.e. for $d\bar{c}_{F,H}/dt = 0$).

In the classical nucleation theory [14–16], the nucleation is represented by the translation of clusters in a phase space of cluster size. Under steady state conditions, the flux of clusters through the size space does not

depend on time and size and can be evaluated to give the steady state nucleation rate in the following form [17]:

$$J_S = \left\{ \sum_{m=1}^{\infty} \frac{1}{W^+(m) f_0(m)} \right\}^{-1},$$
$$f_0(n) = f_0(1) \exp\left\{ -\frac{\Delta G(n)}{kT} \right\}, \tag{3}$$

$$\frac{\Delta G(n)}{kT} = \sum_{m=1}^{n-1} \ln \frac{W^-(m+1)}{W^+(m)}, \tag{4}$$

where $W^+(n)$ and $W^-(n)$ are the forward and backward reaction rates, i.e. the transition rates of n-mer to $(n+1)$-mer or $(n-1)$-mer, respectively, $\Delta G(n)$ is the kinetic analogue of the free energy of forming the n-mer from atoms in a supersaturated solution, known also as the nucleation barrier, kT is Boltzmann's constant times absolute temperature and $f_0(n)$ is the so called constraint equilibrium size distribution function, which describes the size distribution of hetero-phase fluctuations under zero nucleation rate conditions.

For metallic colloids formed by agglomeration of F centers, the forward reaction rate is determined by the rate of F center capture by an n-mer, $\beta_F(n)$, [1] and the backward reaction rate is the sum of the rate of F center loss, $\gamma_F(n)$, and H center capture, $\beta_H(n)$:

$$W^+(n) = \beta_F(n), \qquad W^-(n) = \gamma_F(n) + \beta_H(n). \tag{5}$$

These rates can be found by solving diffusion problem for a colloid with a radius $R_C(n)$ with account of its elastic interaction with PDs [10]

$$\beta_i(n) = \frac{4\pi}{\omega} Z_i^C(n) R_C(n) D_i \bar{c}_i,$$
$$R_C(n) = \left(\frac{3n\omega}{4\pi} \right)^{1/3}, \quad i = F, H, \tag{6}$$

$$\gamma_F(n) = \frac{4\pi}{\omega} Z_F^C(n) R_C(n) D_F c_F^0 \exp\left(\frac{\sigma_{rr}(n)\omega}{kT} \right), \tag{7}$$

where Z_i^C is the capture efficiency of colloids for i-type PD, $i = F, H$ correspond to F and H centers, respectively, $\sigma_{rr}(n)$ is the normal stress at the colloid surface, ω is the atomic volume of the host matrix, D_i are the PD diffusivities, c_F^0 is the thermal equilibrium concentration of F centers near the free surface.

Since the colloids are formed by coagulation of F centers they are expected to be coherent with the host matrix as long as they are small. In this, coherent, state, there exists a misfit, ε, which is equal to the difference between the lattice constants of the colloid crystal lattice and that of the host matrix. In NaCl, considered below in more detail, coherent sodium colloids have a negative misfit (about 7% for fcc- and 4% for bcc-lattices), which means that colloids are under tensile stress given by

$$\sigma_{rr}(n) = \sigma_\varepsilon + \frac{2\gamma_{\text{eff}}}{R(n)}, \quad \sigma_\varepsilon = -\frac{3K_C\varepsilon}{1 + 3K_C/4\mu},$$
$$\gamma_{\text{eff}} = \gamma_C \left(1 + \frac{3K_C}{4\mu} \right)^{-1}, \tag{8}$$

where μ is the shear modulus of the host matrix, K_C is the colloid bulk modulus, and γ_C is the colloid surface free energy.

2.2. Classical nucleation theory

Let us consider first nucleation of colloids from a one-component supersaturated solid solution of F centers, i.e. assume that H centers are not produced, $K_H = 0$, $\bar{c}_H = 0$ and hence $\beta_H(n) = 0$. Then kinetic coefficients entering the forward and backward rates (5) cancel, and the nucleation barrier (4) takes a simple form:

$$\frac{\Delta G(n)}{kT} \xrightarrow[\bar{c}_H \to 0]{} \frac{\Delta G_F(n)}{kT} = \sum_{m=1}^{n-1} \ln \left\{ S_F^{-1} \exp\left(\frac{\sigma_{rr}(m+1)\omega}{kT} \right) \right\},$$
$$S_F = \frac{\bar{c}_F}{c_F^0}, \tag{9}$$

where S_F is the supersaturation, which is determined by the production rate of F centers and the strengths of the F center sinks. Assuming dislocations to be the only sinks present in the initial stage of colloid nucleation (when their number density, N_C, is small) a steady state solution to Eq. (1) is given by

$$\bar{c}_F \xrightarrow[N_C \to 0]{} \frac{K_F}{Z_{F,H}^d \rho_d D_F} \Rightarrow S_F \to \frac{K_F}{Z_{F,H}^d \rho_d D_F c_F^0} = \text{const.} \tag{10}$$

In the continuous (macroscopic) approximation, $n \gg 1$, the sum over m can be evaluated by the integral to give

$$\frac{\Delta G_F(n)}{kT} \approx -n(\ln S_F - \Delta_\varepsilon) + \frac{3}{2} b \left(\frac{4\pi}{3\omega} \right)^{1/3} \alpha_\gamma n^{2/3},$$
$$\alpha_\gamma = \frac{2\gamma_{\text{eff}}\omega}{kTb}, \quad \Delta_\varepsilon = \frac{\sigma_\varepsilon \omega}{kT}, \tag{11}$$

where b is the host lattice atomic spacing.

In the classical nucleation theory, the same expression is obtained by calculating the free energy of n-mer formation, which in the customarily invoked capillarity model consists of the volume and surface parts corresponding to the first and second terms on the right hand side of Eq. (11). $\Delta G(n)$ passes through a maximum at

[1] The thermally activated loss of H centers from colloids (which would also increase their size) can be neglected due to their high binding energy, which is similar to the situation encountered for interstitial atoms in metals.

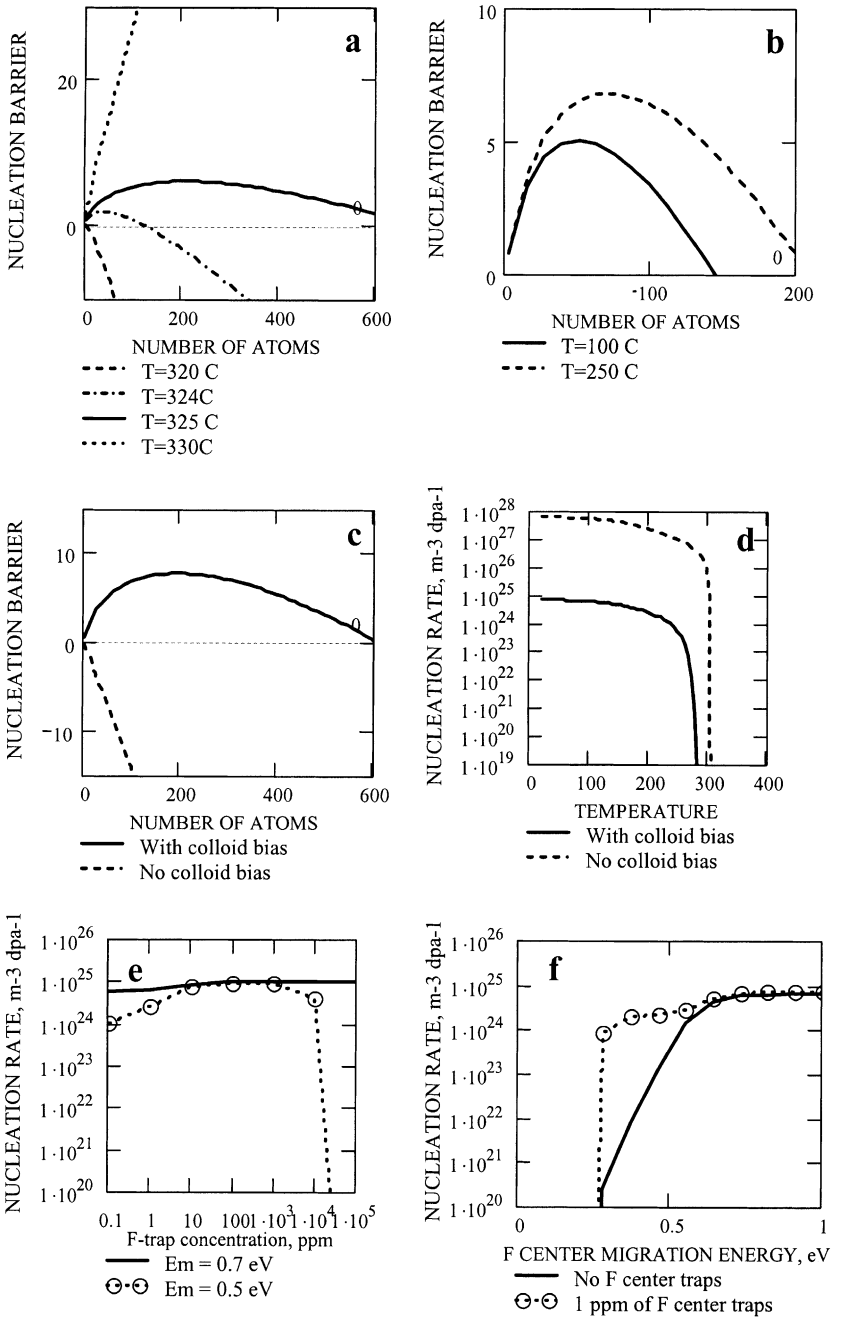

Fig. 2. Nucleation barrier, $\Delta G(n)/kT$ and nucleation rate of colloids at PD production rate $K = 1.3 \times 10^{-5}$ dpa/s: (a) production of F centers alone: strong temperature dependence; (b) simultaneous production of F and H centers: the barrier is purely kinetic at $T \leqslant 100$ °C and it slowly increases with increasing temperature due to increasing evaporation of F centers; (c) effect of the colloid bias on the nucleation barrier and rate at $T = 100$ °C; (d) effect of the colloid bias and temperature on the nucleation rate. Material parameters are given in Table 1; (e) effect of F-trap steady state concentration (measured in atomic parts per million) on the nucleation rate at $T = 100$ °C; (f) effect of F center migration energy on the nucleation rate at $T = 100$ °C.

some critical point n_{crit} as shown in Fig. 2. The critical nucleus is in unstable equilibrium with the supersaturated matrix and has an equal probability of growing or decomposing. Eq. (3) may be evaluated analytically with account of (11) to give the well-known expression for the steady state nucleation rate

$$J_S \xrightarrow[\bar{c}_H \to 0]{} \mathrm{Zeld}\beta_F(1) f_0(1) \exp\left\{ -\frac{\Delta G_F(n_{crit})}{kT} \right\}, \tag{12}$$

$$\mathrm{Zeld} = \left[-\frac{1}{2\pi kT} \frac{\partial^2 \Delta G_F}{\partial n^2}(n_{crit}) \right]^{1/2} = \frac{1}{2\pi (R^F_{crit})^2} \left(\frac{\alpha_\gamma b \omega}{2} \right)^{1/2}, \tag{13}$$

$$\frac{\Delta G_F(n_{crit})}{kT} = \frac{2\pi b}{3\omega} \alpha_\gamma (R^F_{crit})^2, \quad R^F_{crit} = \frac{\alpha_\gamma b}{\ln S_F - \Delta_\varepsilon}, \tag{14}$$

where $f_0(1)$ is the concentration of nucleation sites, Zeld is the Zeldovich factor which is inversely proportional to the width of the fluctuation driven zone in the size space, and R_{crit} is the radius of the critical nucleus. The incubation time needed to establish the steady state nucleation rate is given to a good approximation [18] by

$$\tau \approx [2\beta_F(n_{crit})(\mathrm{Zeld})^2]^{-1} = \frac{\pi (R^F_{crit})^3}{\alpha_\gamma b D_F \bar{c}_F}. \tag{15}$$

2.3. Nucleation under irradiation

The co-precipitation of both F and H centers, which are formed under irradiation, makes it impossible to define the free energy of n-mer formation unambiguously, and consequently the classical nucleation theory should not be used to describe such systems. In the case of void nucleation in metals under irradiation, Katz and Wiedersich [17] and, independently, Russell [18] have shown that the nucleation rate equation is superficially similar to the corresponding equation of classical nucleation theory, in involving a Boltzmann-type factor, but the nucleation barrier is partly kinetic in nature, being a result of the competition between the arrival of vacancies produced in the matrix by irradiation and their thermally activated emission from voids. This barrier vanishes with decreasing irradiation temperature (or increasing dose rate) when the thermal activation becomes negligible. However, as we will show, elastic interaction between voids (or colloids) and arriving PD gives rise to a purely kinetic nucleation barrier, which is determined by material constants and practically does not depend on temperature or dose rate.

Due to their strong elastic interaction with H centers colloids have higher capture efficiency, Z^C_H, for them as compared to that for F centers, Z^C_F, which results in a positive bias for H center absorption by colloids that depends on colloid radius, R_C [10]. Assuming for convenience that $Z^C_F = 1$, the expression for Z^C_H may be written as $Z^C_H(n) = 1 + \delta_C(n)$, where $\delta_C(n)$ is the colloid bias factor:

$$\delta_C(n) = \delta_\varepsilon + \alpha^{im,d} \frac{b}{R_C(n)} + \alpha^{\mu,\xi} \left(\frac{2\gamma_{eff}}{\mu R_C(n)} \right)^2, \tag{16}$$

$$\delta_\varepsilon = \alpha^d (\sigma_\varepsilon/\mu) + \alpha^{\mu,\xi} (\sigma_\varepsilon/\mu)^2, \quad \alpha^{im,d} = \alpha^{im} + \frac{\alpha^d 2\gamma_{eff}}{\mu b}, \tag{17}$$

where δ_ε is the constant 'misfit bias', and the dimensionless bias constants, α, represent different modes of elastic interaction between colloids and PD's [10]. They are defined to be positive as shown in Table 1. It can be seen that the colloid bias increases with decreasing size, and hence for small colloids, the arrival rate of H centers will be higher than that of F centers, which he causes the 'kinetic' nucleation barrier.

Substituting Eqs. (5)–(7) into (4), we can rewrite the latter in the following form

$$\frac{\Delta G(n)}{kT} = \sum_{m=1}^{n-1} \ln \left\{ S^{-1}_{FH} \frac{Z^C_H(m+1)}{Z^C_F(m)} + S^{-1}_F \exp\left(\frac{\sigma_{rr}(m+1)\omega}{kT} \right) \right\},$$
$$S_{FH} = \frac{D_F \bar{c}_F}{D_H \bar{c}_H}, \tag{18}$$

where S_{FH} is the kinetic analogue of the supersaturation in the case of co-precipitation of F and H centers. If H centers are not produced, then $S_{FH} \to \infty$ and we obtain a thermodynamic 'classical' limit considered above.

Let us consider another, purely kinetic, limit $S_F \to \infty$ that corresponds to a complete suppression of the thermal PD's: $c^0_F \to 0$. It determines the nucleation kinetics under irradiation at sufficiently low temperature (or high dose rate) when the thermal PD production becomes negligible. Then, substituting (16) into Eq. (18) and evaluating the sum as we did for Eq. (9) in first approximation for small parameter $b/R_C \ll 1$, we obtain the following expression for the nucleation barrier:

$$\frac{\Delta G_{FH}(n)}{kT} \approx -n(\ln S_{FH} - \delta_\varepsilon) + \frac{3}{2} b \left(\frac{4\pi}{3\omega} \right)^{1/3} \alpha^{im,d} n^{2/3}, \tag{19}$$

which is mathematically equivalent to Eq. (11) and can be obtained from the latter by replacing the thermodynamic constants by their kinetic analogues: $S_F \to S_{FH}$, $\Delta_\varepsilon \to \delta_\varepsilon$, $\alpha_\gamma \to \alpha^{im,d}$.

We are interested in the steady state solution for Eq. (1), $d\bar{c}_{F,H}/dt = 0$, whence it follows that S_{FH} is equal to the ratio of the microstructure sink strengths for H and F centers:

$$S_{FH} \xrightarrow[\text{steadystate}]{} \frac{k^2_H}{k^2_F} = 1 + \delta_{mean}, \quad \delta_{mean} \equiv \frac{k^2_H}{k^2_F} - 1, \tag{20}$$

where δ_{mean} is the mean bias of the microstructure, which evolves in time due to nucleation and growth of ED, and so S_{FH} is not generally a constant. At the initial stage of

Table 1
Material parameters of NaCl and Na colloids used in calculations

Parameter	Value
Irradiation temperature, T, K	373
Dose rate, K, Mrad/h (dpa/s)	240 (1.3×10^{-6})
Maximum dose, Grad (dpa)	500 (100)
Dislocation density, ρ, m^{-2}	10^{14}
Diffusion coefficient of H centers, D_H, $m^2\,s^{-1}$	$10^{-6}\exp(-0.1\ eV/kT)$
Diffusion coefficient of F centers, D_F, $m^2\,s^{-1}$	$10^{-6}\exp(-0.7\ eV/kT)$
Diffusion coefficient of V_F centers, D_v, $m^2\,s^{-1}$	$10^{-6}\exp(-0.69\ eV/kT)$
Formation energy of F centers, E_F^f, eV	1
F–H recombination rate constant, β_r, m^{-2}	10^{20}
NaCl shear modulus, μ, GPa	12.61
Na shear modulus, μ_C, GPa	3.3
Colloid bulk modulus, GPa	6.3
Colloid interface energy, γ_C, J/m^2	0.01
Surface energy of NaCl, γ, J/m^2	0.82
Atomic volume of the host lattice, ω, m^{-3}	4.4×10^{-29}
Ratio of dilatation volumes of H and F centers, $\Omega_H/\lvert\Omega_F\rvert$	3
Dislocation bias, δ_d	0.52
Colloid misfit, ε	0.036–0.068
Misfit bias, δ_ε	0.09–0.24
Elastic-diffusion anisotropy interaction constant, α^d	1
'Image' interaction constant, α^{im}	1
Modulus minus elastic anisotropy interaction constant, $\alpha^{\mu,\zeta}$	30

colloid nucleation, when microstructure is represented by dislocations, one has to good approximation

$$S_{FH} \xrightarrow[N_C \to 0]{} \frac{Z_H^d}{Z_F^d} = 1 + \delta_d, \quad \delta_d \equiv \frac{Z_H^d}{Z_F^d} - 1, \tag{21}$$

where δ_d is the dislocation bias, which is determined by the ratio of relaxation volumes associated with H and F centers, Ω_H/Ω_F [10]:

$$\delta_d = \ln\left(\frac{\Omega_H}{|\Omega_F|}\right) \Big/ \ln\left(\frac{2}{L_H k_H}\right), \quad L_H = \frac{\mu b(1+v)}{3\pi kT(1-v)}\Omega_H, \tag{22}$$

where v is the Poisson ratio, k_H is the square root of the total sink strength of all ED for H centers.

The kinetic (or the bias-induced) nucleation barrier (Fig. 2(b)) is determined by material constants and does not depend on the irradiation conditions, as it is the case for the thermodynamic nucleation barrier (Fig. 2(a)), which is extremely sensitive to the temperature and dose rate.

Under real irradiation conditions, the bias-induced and thermal barriers are effective simultaneously, but the former determines the nucleation rate at sufficiently low irradiation temperature (or high dose rate), a condition where the thermal barrier vanishes (Fig. 2(c)), while the latter determines only the maximum temperature of the colloid formation, above which it increases sharply while suppressing nucleation (Fig. 2(d)).

We have derived analytical expressions for the nucleation barriers and rates for different limiting cases in order to clarify the physical mechanisms of nucleation. Below we will evaluate the nucleation rate numerically by Eqs. (3) and (18) taking into account both bias-induced and thermal effects and making no further approximations.

Fig. 2(d) shows the temperature dependence of the colloid nucleation rate caused by a homogeneous mechanism, i.e. when there are no other nucleation sites except F centers. It can be seen that the homogeneous nucleation rate can be rather high below some threshold temperature but not nearly as high as it would have been in the absence of the bias-induced barrier [17–19] (dashed curve).

Experiments show that small amounts of impurities can have profound effects on the colloid formation in ionic crystals [4–7]. These effects can be modeled by taking into account that impurity ions can act as traps for F centers, which may provide additional (heterogeneous) nucleation sites. On the other hand, F center traps act as recombination sites of F and H centers as well, which decreases a steady-state concentration of F centers (i.e. homogeneous nucleation centers). As a result, the overall effect of such traps on the nucleation rate may depend on their steady state concentration differently for different values of F center migration energy, E_m (Fig. 2(e)). The latter will also depend on the type and concentration of impurity ions, which would strongly affect the nucleation rate, as shown in Fig. 2(f).

3. Nucleation and growth of metallic colloids and halogen bubbles

3.1. Colloids

With increasing irradiation time (or dose), microstructure changes and, generally, one has to solve a time dependent kinetic equation for the size distribution function of the nuclei, which can be written in the form of the Fokker–Planck equation [19,20]:

$$\frac{\partial f(n,t)}{\partial t} = -\frac{\partial}{\partial n}\{f(n,t)(W^+(n,t) - W^-(n,t))\} + \frac{1}{2}\frac{\partial^2}{\partial n^2}\{f(n,t)[W^+(n,t) + W^-(n,t)]\}, \quad (23)$$

where the first term corresponds to the 'drift' flux through the size space and the second term describes 'diffusion' through the size space due to the fluctuations, which are important only in the vicinity of the critical size, $R_{\mathrm{crit}} \pm \Delta R_{\mathrm{C}}$, where the drift part is too small:

$$\Delta R_{\mathrm{C}} = \frac{\omega}{\mathrm{Zeld}4\pi R_{\mathrm{crit}}^2} = \sqrt{\frac{\omega}{2b\alpha^{\mathrm{im,d}}}}. \quad (24)$$

Let us rewrite Eq. (23) in variables R_{C} and t and substitute the second term in (23) by the term describing production of overcritical nuclei of a radius $R_{\mathrm{nucl}} = R_{\mathrm{crit}} + \Delta R_{\mathrm{C}}$:

$$\frac{\partial f(R_{\mathrm{C}},t)}{\partial t} = -\frac{\partial}{\partial R_{\mathrm{C}}}\left\{ f(R_{\mathrm{C}},t)\frac{\mathrm{d}R_{\mathrm{C}}}{\mathrm{d}t}\right\} + \delta(R_{\mathrm{C}} - R_{\mathrm{nucl}})J_{\mathrm{N}}(t), \quad (25)$$

where $J_{\mathrm{N}}(t)$ is the nucleation rate, $\delta(R_{\mathrm{C}} - R_{\mathrm{nucl}})$ is the delta-function, $\mathrm{d}R_{\mathrm{C}}/\mathrm{d}t$ is the colloid growth (or shrinkage) rate. In the low temperature/high dose rate region, in which thermal production of F centers can be neglected, $\mathrm{d}R_{\mathrm{C}}/\mathrm{d}t$ is given by the difference of F and H center influxes, or equivalently, by the difference between the mean bias and the colloid bias that depends on colloid size:

$$\frac{\mathrm{d}R_{\mathrm{C}}}{\mathrm{d}t} = \frac{\omega}{4\pi R_{\mathrm{C}}^2}(W^+ - W^-) \xrightarrow[c_{\mathrm{F}}^0 \to 0]{} \frac{Z_{\mathrm{F}}^{\mathrm{C}} D_{\mathrm{H}} \bar{c}_{\mathrm{H}}}{R_{\mathrm{C}}} \times [\delta_{\mathrm{mean}} - \delta_{\mathrm{C}}(R_{\mathrm{C}})]. \quad (26)$$

3.2. Bubbles

The normal stress at the bubble surface is given by the difference between its surface tension and the gas pressure inside the bubble, P: $\sigma_{rr} = 2\gamma/R_{\mathrm{B}} - P$, where γ is the surface free energy, R_{B} the bubble radius. Accordingly, its bias has both positive and negative contributions that depend on the gas pressure [11]:

$$\delta_{\mathrm{B}}(R_{\mathrm{B}},P) \approx \alpha^{\mathrm{im}}\frac{b}{R_{\mathrm{B}}} + \frac{\alpha^{\mathrm{d}}}{\mu}\left(\frac{2\gamma}{R_{\mathrm{B}}} - P\right) + \frac{\alpha^{\mu,\xi}}{\mu^2}\left(\frac{2\gamma}{R_{\mathrm{B}}} - P\right)^2. \quad (27)$$

Small halogen bubbles have a larger bias for H centers than dislocations or colloids, and hence they will absorb extra H centers and grow via the SIA-loop punching mechanism [11]. With increasing bubble radius beyond some threshold value, R^{th}, its bias decreases very rapidly to the mean bias of the system resulting in the formation of stable bubbles. The stable bubble radius can be only slightly larger and is practically determined by R^{th}, which depends only on the bias parameters as follows [11]:

$$R^{\mathrm{th}} = \frac{4b\alpha^{\mathrm{im}}\alpha^{\mu,\xi}}{4\alpha^{\mu,\xi}\delta_{\mathrm{mean}} + (\alpha^{\mathrm{d}})^2}. \quad (28)$$

The bubble volume fraction, $V_{\mathrm{B}}(t)$ and number density, $N_{\mathrm{B}}(t)$, increase steadily with increasing colloid volume fraction, $V_{\mathrm{C}}(t)$, and are determined by the balance between the amounts of halogen molecules in the bubbles and metal atoms in the colloids [11]:

$$V_{\mathrm{B}}(t) \approx \frac{\omega_{\mathrm{Gas}}}{2\omega}V_{\mathrm{C}}(t), \qquad N_{\mathrm{B}}(t) = \frac{3V_{\mathrm{B}}(t)}{4\pi}\left(R^{\mathrm{th}}\right)^{-3}, \quad (29)$$

where ω_{Gas} is the effective volume per one halogen molecule in a bubble. This implies that by calculating the colloid mean parameters, we will be able to evaluate the bubble parameters as well.

3.3. Simultaneous evolution of colloids and bubbles

Substituting expression (16) into (26) and performing some algebra one can find the critical colloid radius as a function of the mean bias, which changes with time:

$$R_{\mathrm{crit}}(t) = b\left(\frac{1}{2}\frac{\alpha^{\mathrm{im,d}}}{\delta_{\mathrm{mean}}(t) - \delta_{\varepsilon}} + \sqrt{\frac{1}{4}\left(\frac{\alpha^{\mathrm{im,d}}}{\delta_{\mathrm{mean}}(t) - \delta_{\varepsilon}}\right)^2 + \frac{4\gamma_{\mathrm{eff}}^2\alpha^{\mu,\xi}}{(\delta_{\mathrm{mean}}(t) - \delta_{\varepsilon})(\mu b)^2}}\right). \quad (30)$$

If the time to establish a steady state nucleation rate (15) is much less than the characteristic time of variations in the parameter $R_{\mathrm{crit}}(t)$, then the nucleation rate, $J_{\mathrm{N}}(t)$, can be approximated by the steady state expression J_s (3), which changes with time in an adiabatic way, i.e. via variations in δ_{mean}. Then Eq. (25) may be evaluated to give the evolution of the colloid size distribution function and the mean parameters with increasing irradiation dose. The only external parameter in this model is the dislocation density, ρ_{d}. It is known to saturate under irradiation at some value [21], and will is assumed to have a fixed value in our calculations.

Substituting the expression for the mean bias (20) into (30) and neglecting second order corrections in the colloid bias, it is possible to derive a simple analytical expression for the number density of the colloids similar to that for voids in metals [13], which can be presented as a product of two factors, i.e. the material dependent factor N_ρ, that is determined by the dislocation density and other material parameters, and the kinetic factor, $\Phi(t)$, that is determined by the nucleation rate:

$$N_C(t) = N_\rho \Phi(t), \quad N_\rho = \frac{Z_d \rho_d (\delta_d - \delta_\varepsilon)}{4\pi \alpha_c^{im} b},$$

$$\Phi(t) = \left(1 - \frac{R_{crit0}}{R_{crit}(t)}\right)\left(\frac{\overline{R}_C(t)}{R_{crit}(t)} - 1\right)^{-1}, \tag{31}$$

where R_{crit0} is the critical radius at $N_C = 0$ and $\overline{R}_C(t)$ is the colloid mean radius. In the asymptotic limit ($t \to \infty$) and with a fixed value of ρ_d, it can be shown [13] that $R_{crit0}/R_{crit}(\infty) = 0$ and $\overline{R}_C(\infty)/R_{crit}(\infty) \geqslant 1.5$ so that $\Phi(\infty) \leqslant 2$. It means that the asymptotic number density of colloids cannot be larger than the maximum value $N_{RIC} = 2N_\rho$ determined by the RIC mechanism. However, as it is evident from Fig. 3, the colloid ultimate number density is lower than the maximum value, and the difference between the two increases with decreasing nucleation rate.

Fig. 3(a) and (b) show the nucleation rate and number density of colloids calculated for a small colloid misfit parameter, in which case the initial nucleation rate is very high. The number density of colloids saturates rapidly with increasing irradiation dose at values a factor of 3 below N_{RIC}. For low initial nucleation rates (Fig. 3(c) and (d)) the saturation level is lower than N_{RIC} by more than two orders of magnitude, which shows that the asymptotic approximation may be used

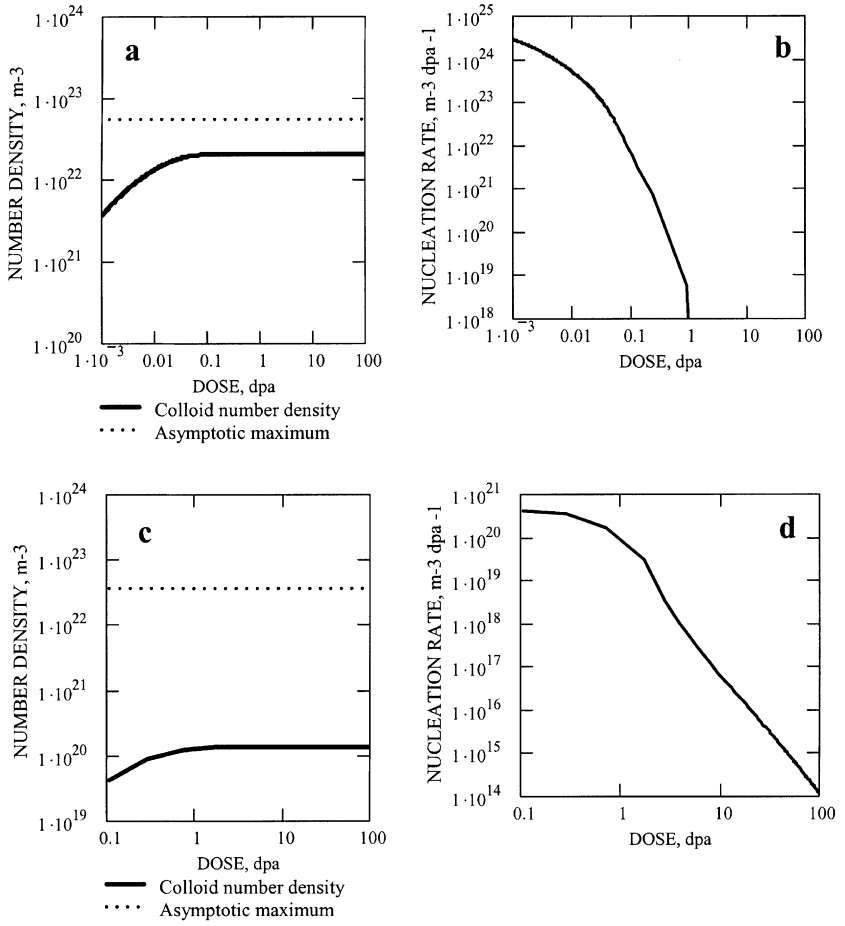

Fig. 3. Number density and nucleation rate of colloids at $K = 1.3 \times 10^{-5}$ dpa/s, $T = 100$ °C, $\rho_d = 10^{14}$ m^{-2}: (a,b) high initial nucleation rate (small colloid misfit, $\varepsilon = 4\%$, 100 appm of F center traps); (c,d) low initial nucleation rate (large colloid misfit, $\varepsilon = 7\%$, no F center traps).

only for a qualitative description of microstructure evolution provided that the nucleation rate is sufficiently high.

4. Void formation and growth in irradiated NaCl

It can be shown [11] that, under particular conditions, colloids grow to sizes exceeding the mean bubble spacing resulting in the direct collisions between them. The amount of energy released in the back reaction is proportional to the energy released due to the formation of one NaCl molecule, and to the number of molecules formed as a result of the collision. The latter is limited by the mean number of chlorine atoms in a bubble, which is about two orders of magnitude smaller than the number of sodium atoms accumulated in a colloid at the time of the collision. The energy released during the back reaction causes an increase of the temperature of the reaction products resulting in an instantaneous and highly localized temperature spike, which is accompanied by an increase of the local pressure up to several GPa [11]. Such a high pressure, although it is extremely short (in the picoseconds range), induces a plastic expansion of the cavity filled with reaction products before it cools down. As a result, we expect the formation of an empty cavity (*void*) in the vicinity of the colloid with a radius exceeding the bubble radius before the collision. This process provides the possibility of explosive formation of voids with sizes exceeding the critical void size, R_{Vcrit}, which can absorb more F centers (as compared to H centers) and grow as a result of their recombination with V_F centers produced at dislocations [10,11]. The overcritical voids will grow faster than colloids (since voids have no misfit bias) and this will provide a mechanism for a next and larger step of explosive back reaction.

According to the present model, the chlorine bubbles are the most finely dispersed ED in the system [10,11] implying that rapidly growing voids start to collide with bubbles first, which would fill them with chlorine gas. One can estimate the gas pressure in voids to be about 5×10^{-3} GPa (50 atm), which is well below the surface tension of the voids [11]. However, the chlorine accumulation within the voids provides the 'fuel' for the explosive back reaction with metallic sodium when growing voids start hitting colloids, which ultimately results in explosion-driven crack formation, if the voids and colloids are large enough [12,22].

The sizes and number densities of colloids and bubbles determine both the onset of the void formation and their 'collision' size. Another important parameter is the number density of voids, which have been measured to range from 10^{19} to 10^{20} m^{-3} in most of our experiments. The void nucleation rate is given by the product of the number of collision between colloids and bubbles per unit time and the probability of formation of an overcritical void in one collision, P_{void}.

$$\frac{\mathrm{d}N_V}{\mathrm{d}t} = \frac{\mathrm{d}V_C}{\mathrm{d}t} N_B P_{\mathrm{void}}. \tag{32}$$

If we assume $P_{\mathrm{void}} = 10^{-3}$ we will obtain the void formation rate observed experimentally.

The bias driven evolution of the system in the case of the bubble–void transition induced by the bubble–colloid collisions is shown in Fig. 4 for two different nucleation rates evaluated at different dislocation densities, concentrations of F-traps and misfit parameters assuming the other parameters to be fixed (Table 1). At the low nucleation rate (Fig. 4(a) and (b)), the resulting colloid volume fraction is low, and the mean intercolloid distance is so large that voids cannot reach the colloids, and material remains stable. This behavior is characteristic for pure NaCl and NaCl doped with 0.04% Br (Fig. 5(a) and (b)).

For the high nucleation rate (Fig. 4(c) and (d)), the resulting colloid number density is very large, and the void and colloid 'collision' sizes are small. This implies that the voids start exploding early but they are not large enough to initiate the void-crack transition, in which case the shape of voids would remain equiaxial [12,22]. This behavior is characteristic for NaCl doped with 0.03% KBF_4 (Fig. 5(c) and (d)).

In the intermediate case, the void 'collision' radius is large enough to initiate the void-crack transition, resulting in the explosive fracture of the material. The materials doped with K, Ba and natural rock salt show this transient behavior (Fig. 5(e) and (f)), and these materials have been shown to be the most susceptible to explosive fracture [7–10,12,22].

5. Discussion and conclusions

We have developed a model of vacancy cluster nucleation and coarsening in irradiated crystals with account of their elastic interaction with PD, which applies for colloid nucleation in ionic crystals and void nucleation in metals. In the latter case, it has been argued [19] that the classical theory of homogeneous void nucleation is not supported by experimental data since it results in void number densities that are several orders of magnitude higher than the usually observed values. This conclusion, in fact, resulted from the modeling of voids as neutral sinks, which they are not. An account of the void bias limits both the nucleation rate and the final number density of voids by the values that are several orders of magnitude lower than those obtained for neutral voids in the technologically important range of high dose rate (or low temperature) irradiation.

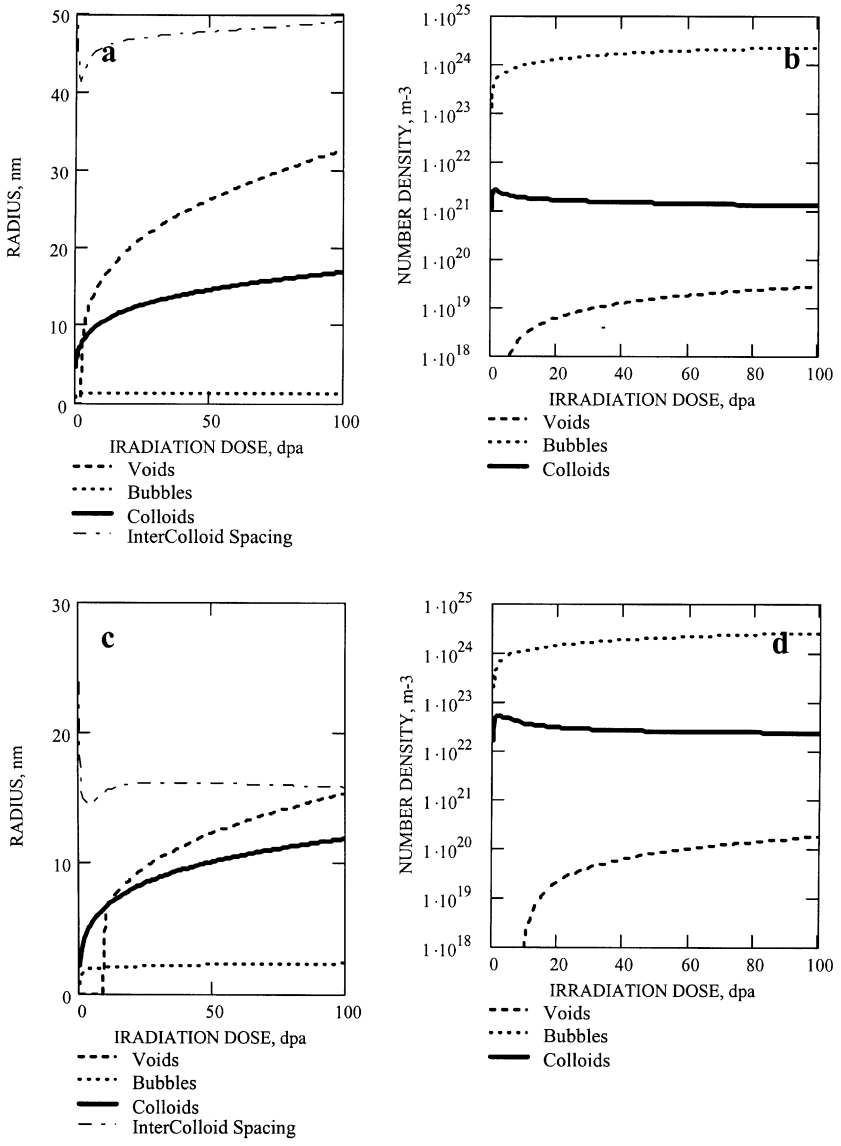

Fig. 4. Evolution of colloids, bubbles and voids at $K = 1.3 \times 10^{-5}$ dpa/s, T = 100 °C: (a,b) low initial nucleation rate ($\varepsilon = 7\%$, no impurity F center traps, $\rho_d = 10^{13}$ m^{-2}); (c,d) high initial nucleation rate ($\varepsilon = 4\%$, 100 appm of impurity F center traps, $\rho_d = 10^{14}$ m^{-2}).

We have applied the model to describe the evolution of sodium colloids, chlorine bubbles and voids in NaCl and have shown that the colloid nucleation kinetics can strongly influence the ultimate response of the material to irradiation. The colloids have been assumed to be coherent with the host matrix, which seems to be likely as long as they are small. However, beyond a certain size, the colloids will lose their coherency, and this change in structural state will strongly affect a subsequent evolution of the microstructure. On the one hand, the intrinsic misfit bias (that is due to the colloid/lattice parameter mismatch) will disappear [10]. On the other hand, incoherent colloids can trap both F and V_F centers, a subsequent recombination of which would produce a 'free' space and, hence, a radiation-induced misfit instead of the intrinsic one, which will result in the colloid bias increase up to the mean microstructure bias and, hence, in a saturation of the colloid growth. At the same time, the increase of the mean bias will provide a possibility for the nucleation of new (coherent) colloids. This transition is expected to take place either after very high irradiation doses [10] or in the case of low initial nucleation rates (Fig. 4(a)), which needs further experimental and theoretical investigations.

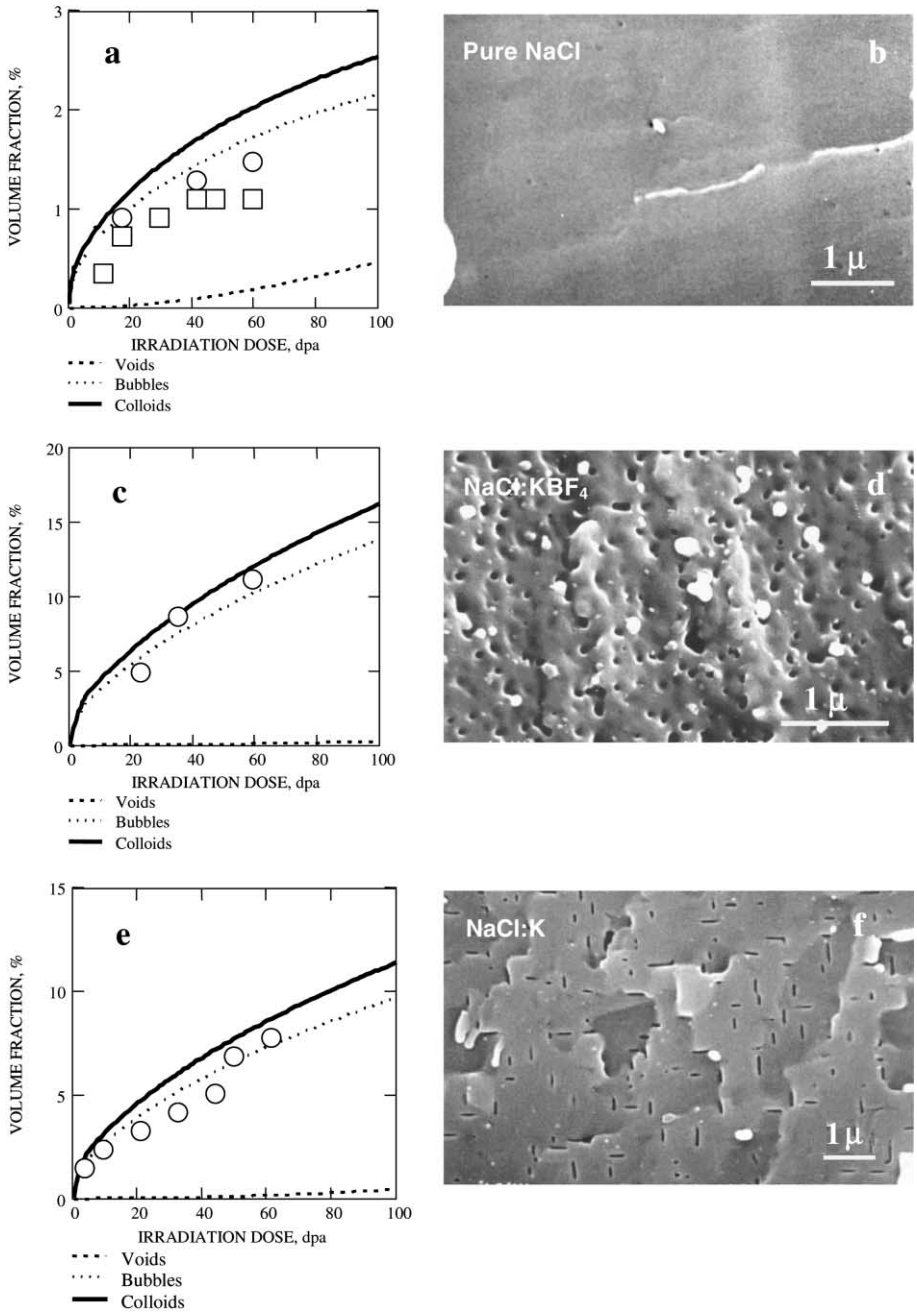

Fig. 5. Comparison of experimental data on the colloid volume fraction vs. irradiation dose for different dopants with theoretical results at $K = 1.3 \times 10^{-5}$ dpa/s, $T = 100$ °C: (a) low initial nucleation rate ($\varepsilon = 7\%$, no F center traps, $\rho_d = 10^{13}$ m^{-2}); circles correspond to measured colloid fraction for pure NaCl, while rectangles correspond to NaCl:Br(0.04 mol%); (b) SEM micrograph of void structure in pure NaCl irradiated to 60 dpa; (c) high initial nucleation rate ($\varepsilon = 4\%$, 100 appm of F center traps, $\rho_d = 10^{14}$ m^{-2}); circles correspond to measured colloid fraction for NaCl:KBF_4 (0.04 mol%); (d) SEM micrograph of void structure in NaCl:KBF_4 (0.04 mol%) irradiated to 60 dpa; (e) intermediate initial nucleation rate ($\varepsilon = 5\%$, 100 appm of F center traps, $\rho_d = 10^{14}$ m^{-2}); circles correspond to measured colloid fraction for NaCl:K(0.1 mol%); (f) SEM micrograph of void structure in NaCl: K(0.1 mol%) irradiated to 60 dpa.

The present results show that the production of radiation damage in heavily irradiated compounds such as NaCl is far more complex than in metals. First, because we are dealing with at least two sub-lattices containing

ions, which are completely different from chemical and mechanical point of view, and secondly, because powerful chemical back reactions might play a significant role in the evolution of microstructure. We have shown that with the theoretical model described in the paper we are able to understand many of the details of the microstructure properties observed for irradiated rock salt samples. These properties include the development of bubbles, colloids and voids, which can be equiaxial or elongated (penny-shaped), while also the observation of explosive back reactions can be understood.

In the present model, we have assumed a constant dislocation density, which seems likely to be the case in ionic crystals similar to that in metals where it is known to saturate with increasing irradiation dose at some value [21]. However, in order to make the theory complete and to obtain comprehensive results, we need to know the dislocation structure dependence on the material parameters and irradiation conditions, which is an outstanding problem of the theory of radiation effects.

Acknowledgements

This study is supported by the NWO-NATO Grant #NB 67-292.

References

[1] U. Jain, A.B. Lidiard, Philos. Mag. 35 (1977) 245.
[2] L.W. Hobbs, A.E. Hughes, D. Pooley, Proc. Roy. Soc. (Lond.) A 332 (1973) 167.
[3] L.W. Hobbs, A.E. Hughes, Radiation Damage in Diatomic Materials at High Doses, Harwell Report AERE-R 8092, 1975.
[4] H.W. Den Hartog, J.C. Groote, J.R.W. Weerkamp, Radiat. Eff. Def. Sol. 139 (1996) 1.
[5] D.I. Vainshtein, C. Altena, H.W. Den Hartog, Mater. Sci. Forum. 239–241 (1997) 607.
[6] H.W. Den Hartog, D.I. Vainshtein, Mater. Sci. Forum. 239–241 (1997) 611.
[7] D.I. Vainshtein, H.W. Den Hartog, Radiat. Eff. Def. Sol. 152 (2000) 23.
[8] D.I. Vainshtein, V.I. Dubinko, A.A. Turkin, H.W. den Hartog, Radiation Eff. Def. Sol. 150 (1999) 173.
[9] V.I. Dubinko, A.A. Turkin, D.I. Vainshtein, H.W. den Hartog, J. Appl. Phys. 86 (1999) 5957.
[10] V.I. Dubinko, A.A. Turkin, D.I. Vainshtein, H.W. den Hartog, J. Nucl. Mater. 227 (2000) 184.
[11] V.I. Dubinko, A.A. Turkin, D.I. Vainshtein, H.W. den Hartog, J. Nucl. Mater. 289 (2001) 86.
[12] D.I. Vainshtein, V.I. Dubinko, A.A. Turkin, H.W. den Hartog, Nucl. Instrum. and Meth. 166&167 (2000) 561.
[13] V.I. Dubinko, P.N. Ostapchuk, V.V. Slezov, J. Nucl. Mater. 161 (1989) 239.
[14] L. Farkas, Z. Phys. Chem 125 (1927) 239.
[15] M. Volmer, Kinetik der Phasenbildung, Stenkopff, 1939.
[16] R. Becker, Anal. Phys. 32 (1938) 128.
[17] J.L. Katz, H. Wiedersich, J. Chem. Phys. 55 (1971) 1414.
[18] K.C. Russell, Acta Metall. 19 (1971) 753.
[19] A.I. Bondarenko, Yu.V. Konobeev, Phys. Stat. Sol. (a) 34 (1976) 195.
[20] L.K. Mansur, in: Kinetics of Nonhomogeneous Processes, Wiley, New York, 1987, p. 377.
[21] F.A. Garner, J. Nucl. Mater. 205 (1993) 98.
[22] A.A. Turkin, V.I. Dubinko, D.I. Vainshtein, H.W. den Hartog, J. Phys.: Condens. Matter 13 (2001) 203.